Determination of the $1s2\ell2\ell'$ state production ratios ${}^4P^o/{}^2P$, ${}^2D/{}^2P$ and ${}^2P_+/{}^2P_-$ from fast ($1s^2$, $1s2s\ {}^3S$) mixed-state He-like ion beams in collisions with H_2 targets

2016 J. Phys. B: At. Mol. Opt. Phys. 49 235202

(http://iopscience.iop.org/0953-4075/49/23/235202)

IOP Publishing Journal of Physics B: Atomic, Molecular and Optical Physics

J. Phys. B: At. Mol. Opt. Phys. **49** (2016) 235202 (12pp) doi:10.1088/0953-4075/49/23/235202

Determination of the $1s2\ell2\ell'$ state production ratios $^4P^o/^2P$, $^2D/^2P$ and $^2P_+/^2P_-$ from fast ($1s^2$, $1s2s\ ^3S$) mixed-state He-like ion beams in collisions with H_2 targets

E P Benis[1] **and T J M Zouros**[2,3]

[1] Department of Physics, University of Ioannina, GR 45110 Ioannina, Greece
[2] Department of Physics, University of Crete, PO Box 2208, GR 71003 Heraklion, Greece
[3] Tandem Accelerator Laboratory, Institute for Nuclear and Particle Physics, NCSR Demokritos, GR 15310 Aghia Paraskevi, Greece

E-mail: mbenis@uoi.gr

Received 9 July 2016, revised 12 September 2016
Accepted for publication 22 September 2016
Published 9 November 2016

Abstract

New results are presented on the ratio $R_m = \sigma_{T_{2p}}(^4P)/\sigma_{T_{2p}}(^2P)$ concerning the production cross sections of Li-like $1s2s2p$ quartet and doublet P states formed in energetic ion–atom collisions by single $2p$ electron transfer to the metastable $1s2s\ ^3S$ component of the He-like ion beam. Spin statistics predict a value of $R_m = 2$ independent of the collision system in disagreement with most reported measurements of $R_m \simeq 1$–9. A new experimental approach is presented for the evaluation of R_m having some practical advantages over earlier approaches. It also allows for the determination of the separate contributions of ground- and metastable-state beam components to the measured spectra. Applying our technique to zero-degree Auger projectile spectra from 4.5 MeV B^{3+} (Benis *et al* 2002 *Phys. Rev.* A **65** 064701) and 25.3 MeV F^{7+} (Zamkov *et al* 2002 *Phys. Rev.* A **65** 062706) mixed state ($1s^2\ ^1S$, $1s2s\ ^3S$) He-like ion collisions with H_2 targets, we report new values of $R_m = 3.5 \pm 0.4$ for boron and $R_m = 1.8 \pm 0.3$ for fluorine. In addition, the ratios of $^2D/^2P$ and $^2P_+/^2P_-$ populations from either the metastable and/or ground state beam component, also relevant to this analysis, are evaluated and compared to previously reported results for carbon collisions on helium (Strohschein *et al* 2008 *Phys. Rev.* A **77** 022706) including a critical comparison to theory.

Keywords: non-statistical population, electron capture, cascade feeding, metastable states, effective solid angle, zero-degree Auger projectile spectroscopy, transfer excitation

(Some figures may appear in colour only in the online journal)

1. Introduction

State-selective information can be obtained from projectile Auger electrons emitted at 0° with respect to the beam direction, where otherwise limiting kinematic broadening is smallest, establishing the zero-degree Auger electron projectile spectroscopy (ZAPS) technique for energetic ions (see [1, 2] and references therein). The use of *pre-excited* long-lived $1s2s\ ^3S$ states, has been particularly attractive to high resolution projectile electron spectroscopy since they can provide a unique and simple *excited* atomic system for testing atomic theory, as for example in single [3–5] and double [6] electron transfer (T), resonant (RTE) and non-resonant (NTE) transfer-excitation (TE) [7, 8], the production of triply-excited states [9] and superelastic scattering [10, 11]. More generally, over the last decade or so, long-lived $1s2s\ ^3S$ states, as found

in mixed ($1s^2$, $1s2s\ ^3S$) state He-like ion beams provided by heavy ion accelerators and highly charged ion sources, have been used in a variety of atomic physics investigations including for example the study of electron impact ionization [12, 13], tokamak high energy charge-exchange [14] and edge impurities [15], electron capture and excitation [16], slow collisions of quasi symmetric heavy systems [17], beam-two-foil spectroscopy [18] and even two-electron quantum entanglement [19]. In most of these cases, it is usually important to accurately know the amount of $1s2s\ ^3S$ metastable fraction, not always easy to obtain within the same measurement.

Recently, interest in ZAPS has been focused on the use of He-like ions in the production of Li-like $1s2s2p\ ^4P$ and ^2P states formed by single $2p$ electron transfer (T_{2p}) to the $1s2s\ ^3S$ metastable state and the determination of the ratio $R_m = \sigma_{T_{2p}}(^4P)/\sigma_{T_{2p}}(^2P)$ of their production cross sections σ in collisions with gas targets [3]. Reports on R_m for carbon [20, 21] and fluorine [3, 22] have found values as large as 9 compared to the predicted spin statistics value of $R_m = 2$ [23], suggesting possible new additional mechanisms at play, such as the proposed *dynamic Pauli exchange* mechanism [3] and/or the *selective cascade feeding* mechanism [20–22].

Here, we present new results on the determination of R_m for additional projectile ions such as boron and fluorine He-like beams in collision with H_2 targets in an effort, not only to extend the isoelectronic focus of these investigations, but also to provide higher accuracy measurements as well. Our ZAPS results are based on a new technique that involves *two* independent measurements of the same electron spectrum at the same collision energy, but using *mixed* beams having quite *different* $1s2s\ ^3S$ metastable beam fraction in each. In the following sections, we present the new technique and show how to extract the distinct contributions from each one of the ground- and metastable-state beam components, thus, separately determining their contributions. In addition, the ratio of $^2P_+/^2P_-$ produced by capture to the metastable component for which spin statistics predicts a 3:1 ratio is also determined for the first time. Finally, we also report on the ratios of $^2D/^2P$ and $^2P_+/^2P_-$ now populated from the $1s^2$ *ground* state beam component by TE and compare them to RTE calculations, thus providing a sensitive indicator as to the importance of RTE and other active TE processes that can affect the overall intensities of the measured Auger spectra. The above ratios are also extracted—using our technique—from the carbon on helium electron spectra presented in [20] and critically compared to those of boron and fluorine, thus extending the isoelectronic database and providing additional information on the basic problem of the unexpected enhancement of R_m.

2. The experimental approach

2.1. ZAPS measurements using mixed $(1s^2\ ^1S, 1s2s\ ^3S)$ state He-like ion beams

The mechanisms for populating the Li-like $1s2l2l'$ doubly excited projectile states depend on the initial state of the ion beam. In tandem accelerators the fast He-like beams are delivered either in: (i) An almost pure ground state ($1s^2\ ^1S$) after *gas* stripping inside the tandem tank [24], (ii) a mixed ($1s^2\ ^1S$, $1s2s\ ^3S$) state, after either stripping the negative ion beam inside the tandem tank or *post*-stripping (by thin carbon foils) the usually Li-like ion beam delivered by the tandem. The value of the metastable fraction $f_{^3S}$ increases with stripping energy reaching a saturation value of about 25%–30% when the stripping velocity of the negative ion beam is near the K-shell electron velocity of the ion v_K [25]. Other shorter-lived states such as the $1s2s\ ^1S$ state, while also initially present in the beam, decay much faster to the ground state and can therefore be safely neglected in the final beam content determination [24].

In figures 1 and 2 we present older ZAPS spectra obtained during our collaboration at the J R McDonald laboratory of Kansas State University. The data were obtained using mixed state ($1s^2\ ^1S$, $1s2s\ ^3S$) He-like ion beams of boron and fluorine in collisions with H_2 measured by a hemispherical deflector analyzer (HDA) with injection lens and position sensitive detector (PSD) [24, 25]. In these two spectra, mixed state ($1s^2\ ^1S$, $1s2s\ ^3S$) beams with quite *different* $f_{^3S}$ values at the *same* collision energy were obtained as judged by the intensity of the observed $1s2s2p\ ^4P$ Auger line. This ^4P state is readily obtained by direct single electron transfer to the metastable component (see discussion in next sections) of the beam and thus is expected to provide an accurate indicator of the beam's $1s2s\ ^3S$ metastable content. As shown in figures 1 and 2, the smaller ratio of ^4P to ^2D yields in spectrum [2] implies, just by visual inspection alone, a significantly smaller fraction, $f_{^3S}^{[2]} < f_{^3S}^{[1]}$ (see also appendix A and equation (A.15)). In the case of F^{7+}, the beam was produced either after post-stripping the incident F^{6+} beam in thin carbon foils or directly from the tandem accelerator after stripping the initial F^- beam in thin carbon foils *inside* the terminal. In the latter case the stripping energy was only 3.2 MeV resulting in a significantly reduced ^4P yield implying a correspondingly much smaller $f_{^3S}$ value, while for the case of foil post-stripping $f_{^3S}$ reaches its maximum value. Similarly, for the B^{3+} case, the maximum value of $f_{^3S}$ was obtained after post-stripping the incident B^{2+} beam in thin carbon foils. A second, smaller $f_{^3S}$ value could be obtained after post-stripping the incident B^{2+} beam in a *gas* post-stripper.

2.2. Technique for the evaluation of $R_m = \sigma_{T_{2p}}(^4P)/\sigma_{T_{2p}}(^2P)$

The determination of R_m in ZAPS measurements so far has involved either *prior* knowledge of the inherent metastable fractions in the impinging ion beam from literature reports [8] or the use of both mixed state ($1s^2\ ^1S$, $1s2s\ ^3S$) and pure $1s^2\ ^1S$ ground state He-like ion beams [3, 20]. In the literature, various methods have been reported for the determination of the metastable $1s2s\ ^3S$ beam fraction including high resolution target K x-ray [26] and low resolution [27] or high resolution projectile Auger [28] or x-ray [29, 30, 31, 32] measurements, as well as more recent ZAPS [24, 25] measurements, in addition to theoretical modeling [33]. Alternatively, carrying out measurements using both pure ground

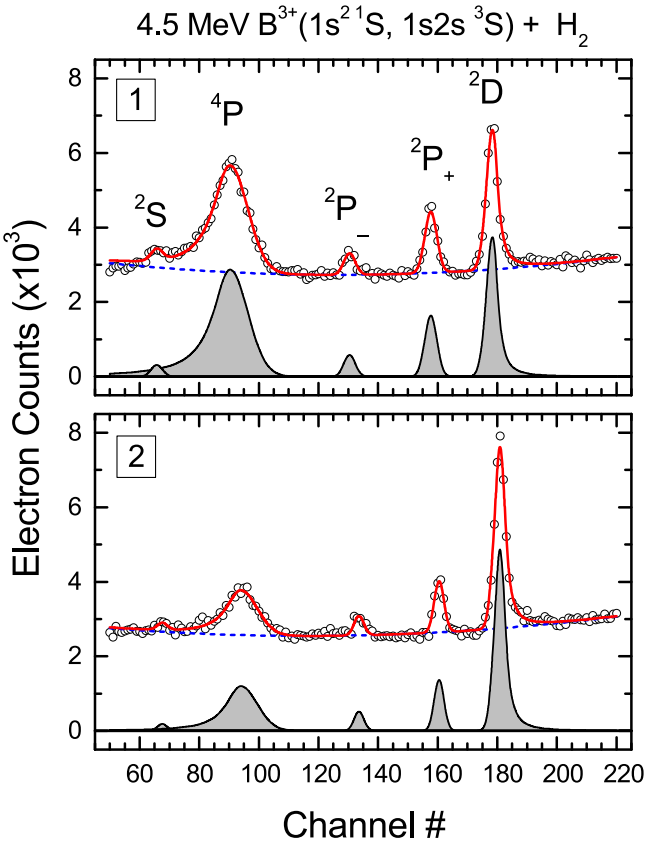

Figure 1. Li-like $1s2l2l'\ ^{(2S+1)}L$ for l, $l' = 0$, 1 (symbolized for short as $^{(2S+1)}L$) Auger electron spectra from 4.5 MeV $B^{3+}(1s^2\ ^1S,\ 1s2s\ ^3S)$ collisions with H_2 as reported in [24]. The B^{3+} beam was produced: [1] after *post*-stripping the incident B^{2+} beam in thin carbon *foils*, [2] after *post*-stripping the incident B^{2+} beam in Ar *gas*. The smaller ratio of ^4P to ^2D yields in spectrum [2] implies $f_{3S}^{[2]} < f_{3S}^{[1]}$. The five peaks have been least square fitted on top of a baseline quadratic background.

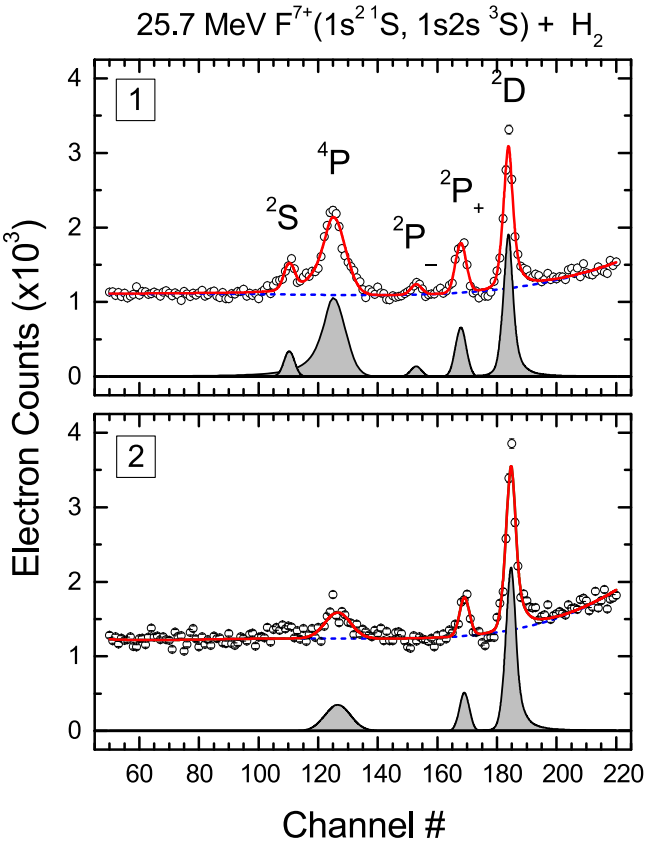

Figure 2. Same as figure 1, but for 25.3 MeV $F^{7+}(1s^2\ ^1S,\ 1s2s\ ^3S)$ collisions with H_2 as reported in [25]. The F^{7+} beam was produced: [1] after *post*-stripping the incident F^{6+} beam in thin carbon *foils*, [2] after *direct* stripping in the tandem accelerator *terminal* the initial F^- beam in thin carbon *foils* at the terminal energy of 3.2 MeV. The significantly reduced ^4P peak observed in spectrum [2] is due to the much lower stripping energy in the terminal.

state and mixed state beams can be quite effective in separating out the processes that originate from the metastable $1s2s\ ^3S$ part of the beam as nicely shown in [20]. However, it is not always possible to obtain near pure (with less than a few percent of metastable) ground state beams utilizing gas stripping inside the tandem tank as f_{3S} depends on the stripping energy. Thus, for measurements in which the stripping energies result in a considerable amount of metastables this method cannot be applied.

Here, we present an approach that addresses the above difficulties, providing an alternative technique that does *not* necessitate the use of a *pure ground state* beam nor the explicit determination of f_{3S}. Instead, it requires *two* measurements of the *same* Auger lines, obtained at the same collision energy, but using a beam of *different* f_{3S} content in each measurement [24]. Below we present this technique in detail after introducing the reader to the necessary definitions.

2.2.1. Definitions. In ZAPS the experimentally determined *electron* double differential cross section (DDCS) in the laboratory at 0° to the beam direction is given by [2, 8]:

$$\frac{\mathrm{d}^2\sigma^e}{\mathrm{d}\Omega\,\mathrm{d}\varepsilon} = \frac{N^e(\varepsilon)}{N_I\, n\, L_c\, \Delta\Omega\, \Delta\varepsilon\, T(\varepsilon)\eta(\varepsilon)}, \tag{1}$$

where N_I is the number of ions collected during the measurement as digitized by a beam current integrator, L_c is the length of the target gas cell, n is the target gas density (molecules cm^{-3}), $\Delta\Omega$ is the effective solid angle, $\Delta\varepsilon$ is the energy resolution, while T and η are the transmission and detection efficiency of the spectrograph, respectively. The number of detected electrons $N^e(\varepsilon)$ is just the 'raw' electron spectrum of counts versus laboratory electron energy ε after background subtraction, which contains the observed Auger lines of the corresponding states x. Here, x corresponds to the 5 lines indicated as $^2S, ^4P, ^2P_-, ^2P_+, ^2D$ in the spectra of figures 1 and 2.

Transformation to the rest frame of the ion (indicated by primed quantities) is given by [34]:

$$\frac{\mathrm{d}^2\sigma^e}{\mathrm{d}\Omega'\,\mathrm{d}\varepsilon'} = \left(\frac{\varepsilon'}{\varepsilon}\right)^{\frac{1}{2}} \frac{\mathrm{d}^2\sigma^e}{\mathrm{d}\Omega\,\mathrm{d}\varepsilon}, \tag{2}$$

$$\varepsilon' = (\sqrt{\varepsilon} - \sqrt{t_p})^2, \tag{3}$$

where ε' is the rest frame electron energy with $t_p = m\,V_p^2/2$ the laboratory kinetic energy of an electron with the same speed V_p as the projectile ion.

Energy integration over each Auger peak x of the spectrum and division by its Auger yield $\xi[x]$ results in the *state production* single differential cross section (SDCS) for each state x:

$$\frac{\mathrm{d}\sigma}{\mathrm{d}\Omega'}[x] = \frac{N^e[x]}{k[x]\,\xi[x]}. \tag{4}$$

Here $N^e[x]$ is just the total number of electrons in the Auger peak x (here determined in a least square fit [35] after background subtraction as shown in figures 1 and 2) divided by the overall absolute 'normalization' constant k for each line given by:

$$N^e[x] \equiv \int_{[x]} N^e(\varepsilon')\mathrm{d}\varepsilon' = \int_{[x]} \left(\frac{\varepsilon'}{\varepsilon}\right) N^e(\varepsilon)\mathrm{d}\varepsilon, \tag{5}$$

$$k[x] \equiv N_I\, n\, L_c\, T\, \overline{\eta}\, \Delta\Omega[x] = \kappa\, G_\tau[x], \tag{6}$$

$$\Delta\Omega[x] = G_\tau[x]\,\Delta\Omega_0, \tag{7}$$

$$\kappa \equiv N_I\, n\, L_c\, T\, \overline{\eta}\, \Delta\Omega_0. \tag{8}$$

Here, $\overline{\eta}$ is now the detection efficiency averaged over the PSD spectrum energy range, while $\Delta\Omega[x]$ is the effective solid angle of the measurement and G_τ a *spectrometer-dependent* solid angle *correction* factor accounting for a possible dependence on the lifetime $\tau[x]$ of the particular state x. It is reminded that the doublet states are all *prompt* therefore having $G_\tau \simeq 1$ and therefore practically the same solid angle $\Delta\Omega_0$, while the ^4P state is *metastable* with $G_\tau \equiv G_\tau[^4P]$ mostly *significantly different* than 1. We have recently computed G_τ for the HDA used in this work [36]. Computations of this correction factor for the two-stage parallel plate analyzer (tandem PPA) have been reported in [2, 8, 20, 37]. The exact value of G_τ is an important correction when measuring the Auger electron yield from the ^4P state for low-Z_p ions and is further discussed below. Finally, $k[x]$ is seen to include the values of all the experimental parameters of the measurement and the accuracy of each of these parameters determines the overall *systematic* uncertainty of the cross section. All the experimental parameters except for G_τ have been collected together into the overall *absolute* normalization parameter κ, which for our HDA has been computed to have an overall *systematic* uncertainty $\Delta\kappa/\kappa \lesssim 0.17$ [38]. We note that κ depends also on the number of recorded ions N_I and can therefore be *very different* from one measurement to the other. Of course, if N_I is the only difference in the two measurements, then the uncertainty will typically be less than 3% with no significant gain in accuracy. However, when the metastable beam fraction is supplied from independently measured fractions using completely different techniques (e.g. x-rays [26]) or apparatus [28] then the uncertainty will be much larger. As shown below, one of the big advantages of computing the *ratio* of peak counts in the *same* measurement (same spectrum) is that κ cancels, thus making the ratio *independent* of κ and the particulars of the experimental set-up and especially the absolute normalization required in cross section determination. This realization is one of the central aspects of our new method involving *ratios* as will become more clear in the next sections.

2.2.2. Determination of the separate contributions from the $1s2s\,^3S$ and $1s^2\,^1S$ states. For an electron spectrum obtained from a mixed state beam, with contributions to the Auger line x from *both* the $1s^2\,^1S$ ground (g) and $1s2s\,^3S$ metastable (m) states we may write quite generally [8]:

$$N^e[x] = N_m^e[x] + N_g^e[x] \tag{9}$$

$$= k[x]\,\xi[x]\left[\frac{N_g}{N_I}\left(\frac{\mathrm{d}\sigma_g[x]}{\mathrm{d}\Omega'}\right) + \frac{N_m}{N_I}\left(\frac{\mathrm{d}\sigma_m[x]}{\mathrm{d}\Omega'}\right)\right] \tag{10}$$

or equivalently using the results of equation (4):

$$\frac{\mathrm{d}\sigma[x]}{\mathrm{d}\Omega'} = (1 - f_{^3S})\left(\frac{\mathrm{d}\sigma_g[x]}{\mathrm{d}\Omega'}\right) + f_{^3S}\left(\frac{\mathrm{d}\sigma_m[x]}{\mathrm{d}\Omega'}\right). \tag{11}$$

Here, the total number of accumulated ions N_I is the sum of the ions in the ground state N_g and metastable state N_m, i.e. $N_I = N_g + N_m$, while the metastable fraction $f_{^3S}$ is defined as $f_{^3S} \equiv N_m/N_I$ [24]. In this case, $\mathrm{d}\sigma_g[x]/\mathrm{d}\Omega'$ and $\mathrm{d}\sigma_m[x]/\mathrm{d}\Omega'$ represent the differential production cross sections for *all* possible processes that can populate the state x from either the ground state (g) or metastable states (m) and are by the above definition *independent* of the amount of metastable fraction in the utilized ion beam. This is clearly *not* the case for $\mathrm{d}\sigma[x]/\mathrm{d}\Omega'$ which is strictly dependent on the amount of metastable fraction $f_{^3S}$ as shown explicitly in equation (11). It is therefore not a real cross section as such.

Since we shall be interested in two different measurements $i = 1, 2$ each with a different amount of metastable fraction $f_{^3S}^{[i]}$, for a measurement i, we may write:

$$\frac{\mathrm{d}\sigma_i[x]}{\mathrm{d}\Omega'} = \left[(1 - f_{^3S}^{[i]})\left(\frac{\mathrm{d}\sigma_g[x]}{\mathrm{d}\Omega'}\right) + f_{^3S}^{[i]}\left(\frac{\mathrm{d}\sigma_m[x]}{\mathrm{d}\Omega'}\right)\right] \tag{12}$$

$$\text{for } x:\ {}^2P_{\pm}, {}^4P,\ {}^2D.$$

Thus, for two independent measurements $i = 1, 2$, equations (12) lead to 2 equations for each one of the 4 states ($^2P_{\pm}$, ^4P or ^2D) and therefore to a total of eight equations with ten unknowns: the two metastable fractions $f_{^3S}^{[1]}, f_{^3S}^{[2]}$, and each of the four contributions from the ground $\frac{\mathrm{d}\sigma_g[x]}{\mathrm{d}\Omega'}$ and four from the metastable $\frac{\mathrm{d}\sigma_m[x]}{\mathrm{d}\Omega'}$ beam components. This system of simultaneous nonlinear equations *cannot* be solved. However, as discussed in section 3, under the assumptions that the ^4P state is populated predominantly from the metastable state (by direct electron transfer) and the ^2D state is populated predominantly from the ground state (by TE) we set $\frac{\mathrm{d}\sigma_g[^4P]}{\mathrm{d}\Omega'} \simeq 0$ and $\frac{\mathrm{d}\sigma_m[^2D]}{\mathrm{d}\Omega'} \simeq 0$, eliminating two of the unknowns in the system of equations (12). This simplification allows for the system to be solved—see equations (A.12) and (A.13) in appendix A)—which are written here in the more

compact form:

$$\frac{\mathrm{d}\sigma_m[x]}{\mathrm{d}\Omega'} = S[^2D]H[x,\ ^2D] \quad \text{for } x:\ ^2P_{\pm},\ ^4P,\ ^2D \tag{13}$$

$$\frac{\mathrm{d}\sigma_g[x]}{\mathrm{d}\Omega'} = S[^4P]H[x,\ ^4P] \tag{14}$$

with

$$S[x] \equiv \frac{\mathrm{d}\sigma_1[x]\mathrm{d}\sigma_2[x]}{\mathrm{d}\sigma_2[x] - \mathrm{d}\sigma_1[x]}, \tag{15}$$

$$H[x,\ y] \equiv \left(\frac{\mathrm{d}\sigma_1[x]}{\mathrm{d}\sigma_1[y]} - \frac{\mathrm{d}\sigma_2[x]}{\mathrm{d}\sigma_2[y]}\right), \tag{16}$$

where we have used the short hand $\mathrm{d}\sigma_i[x] \equiv \mathrm{d}\sigma_i[x]/\mathrm{d}\Omega'$. We may further express H using equation (4) which together with equation (6) gives:

$$H[x,\ ^4P] = \frac{G_\tau\,\xi[^4P]}{\xi[x]}N[x,\ ^4P] \tag{17}$$

so that

$$H[^4P,\ ^2D] = \frac{\xi[^2D]}{G_\tau\,\xi[^4P]}N[^4P,\ ^2D], \tag{18}$$

$$H[^2P_{\pm},\ ^2D] = \frac{\xi[^2D]}{\xi[^2P_{\pm}]}N[^2P_{\pm},\ ^2D] \tag{19}$$

with

$$N[x,\ y] \equiv \left(\frac{N_1^e[x]}{N_1^e[y]} - \frac{N_2^e[x]}{N_2^e[y]}\right). \tag{20}$$

We note here that $N[x,\ y]$ has the important property that it is *independent* of any absolute normalization parameters of the measurement as for example those included in $k[x]$ given in equation (6). It is simply composed of ratios of raw counts (areas under the peaks) from the *same* spectrum, as shown in the examples of figures 1 and 2.

2.2.3. Ratios R_m, r_m, R_g and r_g. The main ratio of interest to this study and also measured in other works is the ratio R_m of ^4P to ^2P contributions from the *metastable* $1s2s\ ^3S$ component of the beam. Here, we also include the determination of three additional ratios which should provide further consistency checks as well as further insight into the model assumptions. These ratios include the ratio r_m of $^2P_+$ to $^2P_-$ contributions from the metastable $1s2s\ ^3S$ which according to theory should be 3:1 [39]. In addition, we also define ratios of contributions from the *ground* state $1s^2\ ^1S$ component, R_g of ^2D to ^2P and r_g of $^2P_+$ to $^2P_-$ states. The contributions to these ground state ratios arise from TE, which theory is expected to be able to calculate within about 20% when the process is resonant (RTE) [8].

The ratios R_m, R_g and r_m and r_g are defined here as follows:

$$R_m \equiv \frac{\dfrac{\mathrm{d}\sigma_m[^4P]}{\mathrm{d}\Omega'}}{\dfrac{\mathrm{d}\sigma_m[^2P_+]}{\mathrm{d}\Omega'} + \dfrac{\mathrm{d}\sigma_m[^2P_-]}{\mathrm{d}\Omega'}}, \tag{21}$$

$$R_g \equiv \frac{\dfrac{\mathrm{d}\sigma_g[^2D]}{\mathrm{d}\Omega'}}{\dfrac{\mathrm{d}\sigma_g[^2P_+]}{\mathrm{d}\Omega'} + \dfrac{\mathrm{d}\sigma_g[^2P_-]}{\mathrm{d}\Omega'}}, \tag{22}$$

$$r_m \equiv \frac{\dfrac{\mathrm{d}\sigma_m[^2P_+]}{\mathrm{d}\Omega'}}{\dfrac{\mathrm{d}\sigma_m[^2P_-]}{\mathrm{d}\Omega'}}, \tag{23}$$

$$r_g \equiv \frac{\dfrac{\mathrm{d}\sigma_g[^2P_+]}{\mathrm{d}\Omega'}}{\dfrac{\mathrm{d}\sigma_g[^2P_-]}{\mathrm{d}\Omega'}}. \tag{24}$$

Using the results of equations (13) and (14) we may evaluate the four ratios to obtain:

$$R_{m\,\mathrm{exp}} = \frac{\dfrac{N[^4P,\ ^2D]}{G_\tau\,\xi[^4P]}}{\dfrac{N[^2P_+,\ ^2D]}{\xi[^2P_+]} + \dfrac{N[^2P_-,\ ^2D]}{\xi[^2P_-]}}, \tag{25}$$

$$R_{g\,\mathrm{exp}} = \frac{\dfrac{N[^2D,\ ^4P]}{\xi[^2D]}}{\dfrac{N[^2P_+,\ ^4P]}{\xi[^2P_+]} + \dfrac{N[^2P_-,\ ^4P]}{\xi[^2P_-]}}, \tag{26}$$

$$r_{m\,\mathrm{exp}} = \frac{\xi[^2P_-]}{\xi[^2P_+]}\,\frac{N[^2P_+,\ ^2D]}{N[^2P_-,\ ^2D]}, \tag{27}$$

$$r_{g\,\mathrm{exp}} = \frac{\xi[^2P_-]}{\xi[^2P_+]}\,\frac{N[^2P_+,\ ^4P]}{N[^2P_-,\ ^4P]}. \tag{28}$$

All four ratios are seen in equations (25)–(28) to be expressed as functions of $N[x,\ y]$ (defined in equation (20)) in which the absolute normalization parameters κ have canceled and therefore all four ratios depend only on the areas $N_i^e[x]$. Also *not* required is the knowledge of the metastable fraction in each measurement $i = 1,\ 2$ something not immediately obvious from the form of the equations involving the cross sections $\mathrm{d}\sigma_m/\mathrm{d}\Omega'$ and $\mathrm{d}\sigma_g/\mathrm{d}\Omega'$ in appendix A.

Clearly, this is a considerable advantage since both the absolute normalization and metastable fraction determination is in general more tedious to obtain requiring special attention to additional experimental details. In the case of the ratios $R_{m\,\mathrm{exp}}$ and $r_{m\,\mathrm{exp}}$, it is also clear that the Auger yields, $\xi[^2D]$, cancel, but not so for the ratios $R_{g\,\mathrm{exp}}$ and $r_{g\,\mathrm{exp}}$. Thus, except for the theoretically determined P state Auger yields $\xi[^2P_{\pm}]$ needed in all ratios, only the solid angle correction factor G_τ and Auger yield $\xi[^4P]$ is needed for $R_{m\,\mathrm{exp}}$, while both Auger

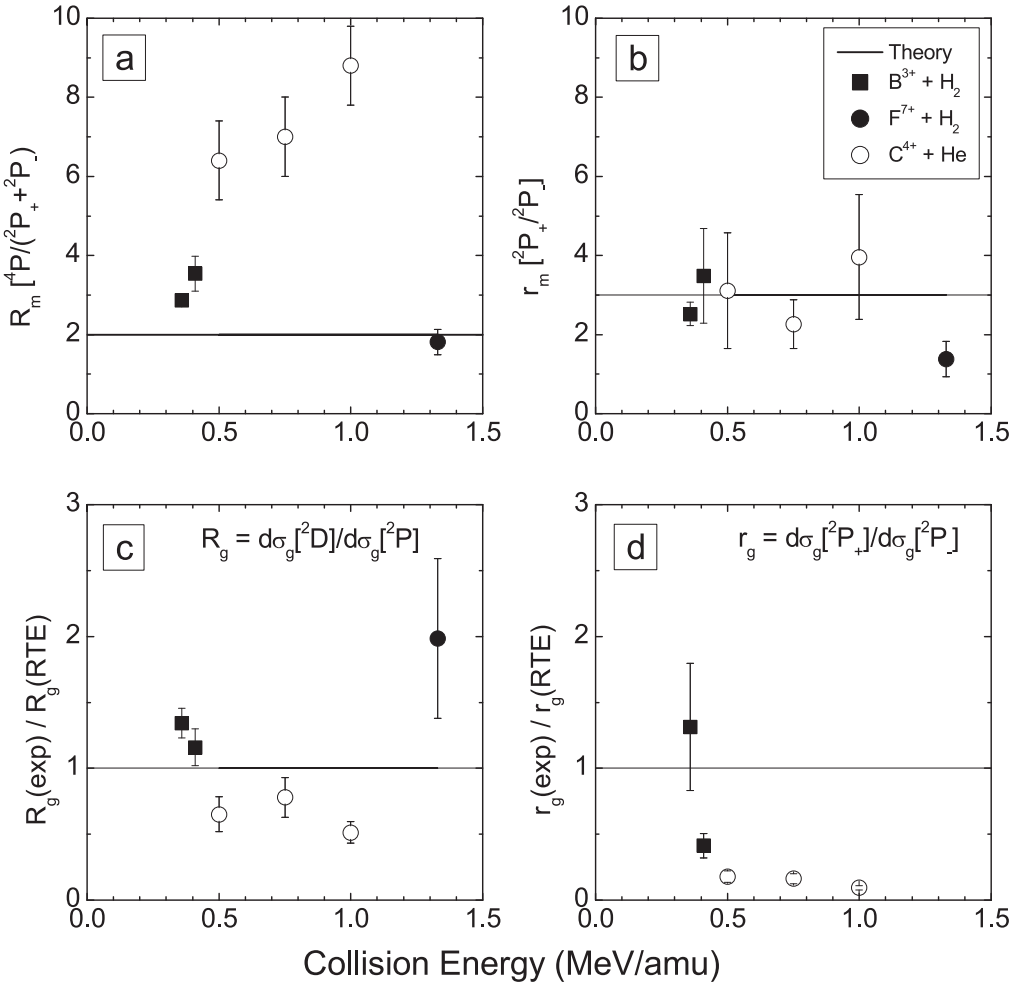

Figure 3. Theoretical results are compared to experimental ratios obtained using the two spectra approach from two distinct measurements with different metastable content. This work: (filled squares) 4 MeV B^{3+} and 4.5 MeV B^{3+} on H_2 (from spectra reported in [24] with the 4.5 MeV case shown in figure 1), (filled circles) 25.3 MeV F^{7+} on H_2 (from spectra reported in [25] and shown in figure 2). Also shown for comparison (open circles) are results obtained from the spectra reported in [20]. (a) and (b) show the ratios $R_{m,\mathrm{exp}}$ and $r_{m,\mathrm{exp}}$ as computed by equations (25) and (27) using the fitted areas of the boron and fluorine spectra. The theory lines represent the predictions of single electron capture to the metastable state, i.e. $R_{m,\mathrm{theo}} = 2$ and $r_{m,\mathrm{theo}} = 3$ [39]. (c) and (d) show ratios $R_{g,\mathrm{exp}}$ and $r_{g,\mathrm{exp}}$ similarly computed using equations (26) and (28) compared to RTE calculations. The fluorine data point for r_m is missing as the $^2P_-$ counts are practically zero as can also be seen in the spectrum itself (figure 2).

yields $\xi[^4P]$ and $\xi[^2D]$, but not G_τ is needed in $R_{g\,\mathrm{exp}}$. Otherwise *no* additional theoretical or experimental parameters are needed. Moreover, since the angular distributions of the Auger decays from the ^4P and ^2P states can be expected to be quite similar (both are P states), $R_{m\,\mathrm{exp}}$ practically corresponds to the ratio $\sigma_m[^4P]/\sigma_m[^2P]$ of the *total* production cross sections.

Finally, the metastable fractions $f_{^3S}^{[1]}$ and $f_{^3S}^{[2]}$ of each measurement can also be obtained *self-consistently* within the same method. These can also be written in terms of the raw counts as:

$$f_{^3S}^{[i]} = \frac{N_i^e[^4P]}{\kappa_i}\left[\frac{\kappa_1 N_2^e[^2D] - \kappa_2 N_1^e[^2D]}{N_2^e[^2D]N_1^e[^4P] - N_1^e[^2D]N_2^e[^4P]}\right] \quad (i = 1, 2) \tag{29}$$

which are essentially the same as the expressions given in [24]. In this case, however, we note the existence of the absolute normalization parameters κ_i. Thus, in the case of the metastable fraction determination the relative calibration (ratio of κ_2/κ_1) is necessary. The expressions for the metastable fractions, however, are seen to be *independent* of the Auger yields ξ as expected, but also of the correction factor G_τ which cancels since $N_i^e[^4P]$ appears both in the numerator and denominator of equations (29) [24].

In figure 3, we present experimental results for the four ratios as extracted from the fits to the boron and fluorine spectra shown in figures 1 and 2, respectively. In addition, for comparison we have also included the R_m results for carbon on helium spectra from [20], for which values of R_m were found to lie in the range of 6–9, as well as values for the other three ratios r_m, R_g and r_g calculated with our method. These results are discussed next in section 3.

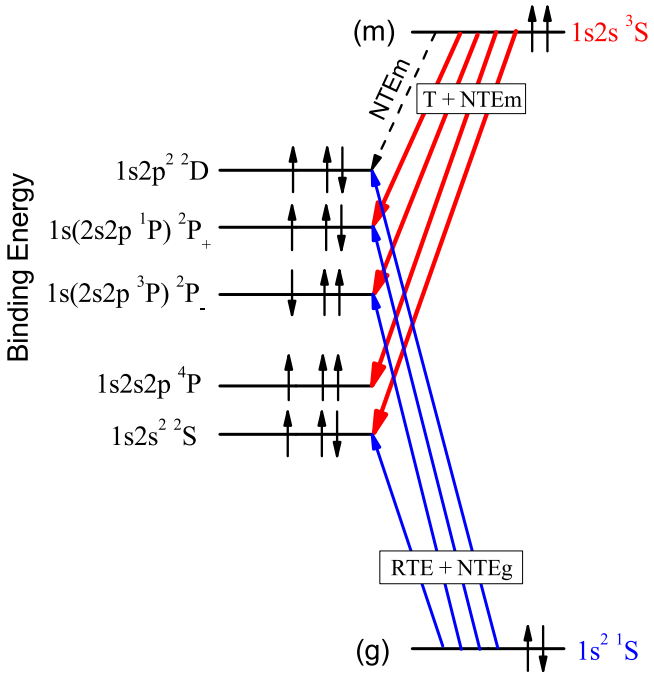

Figure 4. Energy level diagram showing the dominant mechanisms for the production of the $1s2l2l'\ ^{(2S+1)}L$ doubly excited states formed in collisions of energetic He-like ($1s^2\ ^1S$, $1s2s\ ^3S$) beams with H_2 targets. Single $2p$ or $2s$ electron transfer (T) or non-resonant transfer excitation (NTEm) to the metastable state (m) in red, transfer and excitation (both resonant (RTE) and non-resonant (NTEg)) from the ground state (g) in blue (for more details see text).

3. Results and discussion

3.1. Dominant processes

The *dominant* processes involved in the population of the $1s2l2l'\ ^{(2S+1)}L$ doubly excited states during collisions of energetic He-like ($1s^2\ ^1S$, $1s2s\ ^3S$) ions with H_2 targets are illustrated in figure 4. As shown, all the doublet states can be populated (a) from the ground state via the processes of RTE and NTE [7, 23] and (b) from the metastable state via NTE. RTE is prohibited in case (b) due to energy conservation considerations. Here we refer collectively to NTEg to designate all NTE processes from the ground state and to NTEm to designate all NTE processes from the metastable state.

The ^4P state cannot be populated from the ground state by NTEg processes due to spin conservation selection rules [3, 22] and only negligibly so by RTE since the ^4P Auger rate is orders of magnitude smaller than for the ^2P and ^2D states. Other possible population processes from the ground state would involve the $1s$ ionization followed by double electron transfer to the $2s$ and $2p$ states or an NTEg process with spin flip. Both cases are in principle viable if targets with more than two electrons are used, but all are of higher order compared to single electron transfer and consequently can be considered much weaker and neglected. Moreover, they can be safely excluded from this study since only H_2 targets are considered. Alternatively, the $1s2s\ ^3S$ state contributes to the population of the ^4P state through the processes of NTEm and T_{2p} [4]. As stated, the RTE process is prohibited for this state, as also for the ^2P states, due to energy conservation considerations [8]. It is documented in the literature that the NTEm process is negligible compared to T_{2p} when using H_2 targets, for both ^2P and ^4P states, for collision energies of 0.5–1 MeV/u which are considered here [8]. Thus, under the above stipulations, the ^4P state is populated primarily via the T_{2p} process to the metastable $1s2s\ ^3S$ state, while the ^2P state by either RTE from the $1s^2$ ground state and/or T_{2p} from the $1s2s\ ^3S$ state.

The case of the ^2D state is special since it is strongly populated by RTE from the ground state in the present energy range. Indeed, according to the impulse approximation (IA) [8], the RTE maximum for the ^2D states in collisions with H_2 is at $E_R \simeq 3.65$ MeV for boron and $E_R \simeq 19.6$ MeV for fluorine. Thus, for the collision energies reported in this work and when using an H_2 target, RTE is expected to be dominant in the formation of the ^2D state [7, 8] ruling out contributions from NTEg and NTEm (just T_{2p} is not viable) as negligible.

It is important to realize that our technique (as well as that of [20]) approximates the original definition of R_m as the ratio of *single* $2p$ *electron transfer* cross sections $\sigma_{T_{2p}}(^4P)/\sigma_{T_{2p}}(^2P)$ by the ratio of *metastable* SDCS as expressed by equation (21) and evaluated from the experimental data by equation (25). Since both T_{2p} and NTEm are in principle viable from the metastable state (they are not distinguishable in ZAPS) as shown in figure 4, our approximation holds only if NTEm is much smaller than T_{2p}, as is the case for the collision systems investigated here. However, this might not always be the case, as for example with heavier targets and/or at lower collision energies, where due care must always be exercised. More investigations of this point are clearly needed both theoretical and experimental.

3.2. Evaluation of ratios R_m and r_m

We now apply equations (21) and (23) to compute R_m and r_m for the spectra of figures 1 and 2. For 25.3 MeV fluorine collisions with H_2, the value obtained is $R_{m\,\mathrm{exp}} = 1.8 \pm 0.3$ which is very close to the statistically expected value of $R_m = 2$. This $R_{m\,\mathrm{exp}}$ value is also in qualitative agreement with the Auger spectra of Lee *et al* [8] analyzed in [22]. It is worth noting that the Lee *et al* [8] fluorine ZAPS results, were obtained using a tandem PPA placed much closer to the gas target (than in the case of our HDA), very similar to the setup used in [20] for carbon. Furthermore, in the analysis of Lee *et al* the metastable fraction was *not* measured *in situ* (this technique to measure the metastable fraction only became known much later [24]), but was taken from the even older high resolution Auger measurements of Dillingham *et al* obtained with an entirely different apparatus [28] and thus could in fact be quite different. Our new fluorine $R_{m\,\mathrm{exp}}$ result does not seem to support the need for any mechanisms enhancing the population of the ^4P state which of course could be quite different at lower collision energies where much larger R_m values were reported [22]. On the contrary, for the case of boron, $R_{m\,\mathrm{exp}} = 3.5 \pm 0.4$, well above the statistically expected value of $R = 2$. Moreover, the value for boron is in accordance with the value of $R_{m\,\mathrm{exp}} = 2.9 \pm 0.2$,

recently reported for collisions of 4 MeV $B^{3+}(1s^2\ ^1S, 1s2s\ ^3S)$ with H_2 targets [40], utilizing the method of [20].

Any enhancements of $R_{m\,\mathrm{exp}}$ above the value of two must be accounted either by increasing the numerator leading to the enhancement of the ^4P population or by decreasing the denominator leading to the depression of the ^2P population. To date, two different mechanisms increasing the numerator both feeding the metastable $1s2s2p\ ^4P$ state have been proposed to account for the observed enhancements: (a) The *Pauli exchange interaction* where a target electron which is spin-aligned with the two projectile electrons in the $(1s2s\ ^3S)$ state experiences a (slightly) different potential than an anti-aligned electron. If the interaction potentials are different, the outcomes (^4P versus ^2P formation) could also be different. This process does not necessarily involve the excitation of the projectile $1s$ electron and could possibly be described within the independent electron model, but one would need spin-dependent potentials—a difficult task—not yet attempted [41]. It is expected to result in additional ^4P population [3, 20, 21]. It was first suggested in an effort to explain the value $R_{m\,\mathrm{exp}} = 2.9$ seen in measurements of 1.1 MeV/u fluorine in collisions with He [3] and later on for the even larger values $R_{m\,\mathrm{exp}} = 6$–9 for 0.5–1.5 MeV/u collisions of carbon on He [20, 21]. (b) The *selective cascade feeding* of the $1s2s2p\ ^4P$ state from higher lying $1s2snl\ ^4L$ states (formed by nl electron transfer with $n > 2$) through strong radiative $E1$ transitions between quartets, eventually transferring the extra nl population to the $1s2s2p\ ^4P$ [20–22]. The higher lying $1s2snl\ ^2L$ states can also be formed by nl electron transfer, but in this case they preferentially decay strongly by Auger transitions allowing for negligible feeding of the $1s2s2p\ ^2P$ states [21, 22].

In addition, a third process is considered here that merits further investigation: the blending of the $1s2p^2\ ^4P^e$ line, not yet discussed so far, with the $^2P_+$, as it gives rise to an Auger electron with almost the same energy [5, 42]. What holds for the production of the $1s2s2p\ ^4P$ should also apply for the $^4P^e$ state. For low-Z targets such as H_2 and He, the $^4P^e$ line can only be populated by NTEm, in a way similar to the $1s2p^2\ ^2D$ line, but probably much weaker. Thus, if significant, possibly at lower collision energies where NTEm is strongest, it could lead to an overestimation of what has been considered so far to be a *pure* $^2P_+$ line, but actually might include the blended contributions of both $^4P^e$ and $^2P_+$ lines. Their energy difference is probably beyond the limits of ZAPS (differences less than ~0.1%), but taking advantage of the soft metastability of the $^4P^e$ (mean lifetime 0.1–1 ns [42]) some possibilities might still exist for its extraction from under the otherwise prompt $^2P_+$ line and check its intensity [43]. As a contra indication we might note that this line blending would increase the ratio r_m of $\sigma_{T_{2p}}(^2P_+)/\sigma_{T_{2p}}(^2P_-)$ expected to be 3 by spin statistics [23], so far in accord with recent observations [40].

Next we consider the ratio r_m, which as does R_m, should also test how well single $2p$ electron capture to the metastable state obeys spin statistics. As already stated theory predicts the ratio for $2p$ capture to the metastable state should form the states ^4P, $^2P_-$ and to $^2P_+$ in the ratios 8: 1: 3 and therefore $r_m = 3$. This is seen to be in fair to good agreement with the experimentally determined ratios reported in figure 3(b) with the exception of the 25.3 MeV fluorine data which is seen to be a bit smaller at $r_{m\,\mathrm{exp}} = 1.4 \pm 0.5$.

Finally, in figure 3, we also include the values of $R_{m,\mathrm{exp}}$ extracted from fits to the subtracted spectra of [20] (figure 5) using *their* reported solid angle corrections factors. Our extracted values for $R_{m,\mathrm{exp}}$ were 9 ± 1, 9 ± 1 and 10 ± 1 for 6, 9 and 12 MeV, respectively, which though a bit higher than those reported in [20], are still within the reported experimental errors. For the sake of consistency in figure 3(a) we have plotted the values given in the original reference. For the determination of the $r_{m,\mathrm{exp}}$ ratio though, we used fitted areas to the unsubtracted spectra of [20] (figure 2). It is clearly seen that our measurements and those of [20] are in fair agreement as to the determination of the ratio r_m. However, a quite large disagreement is evident for the ratio R_m. The main difference in the evaluation of R_m as compared to r_m is the determination of the effective solid angle factor G_τ. As already mentioned, the detection solid angle of the quartet and doublet states can be very different resulting in a considerable correction [2, 4] which is quite sensitive to the particulars of the experimental setup and the spectrometer used in the measurement. Measurements of [20] were obtained with the tandem PPA, while in our measurements we used an HDA equipped with an injection lens. In our case the effective solid angle was accurately determined in a Monte Carlo type approach within the SIMION8.1 ion optics package [36], while for the tandem PPA only purely geometrical calculations were applied raising questions about the accuracy of the computed correction. Thus, the solid angle correction factor could in fact be a possible source of significant systematic error in the determination of $R_{m,\mathrm{exp}}$ in [20]. It is our intention to try to determine it in a similar way as we did for the HDA [36], in a future investigation.

3.3. Evaluation of ratios R_g and r_g

The ratios R_g and r_g refer to ratios of contributions from the *ground* state which according to the preceding discussion and figure 4 are expected to occur primarily via the TE process. For H_2 targets, and to a slightly lesser extent for He targets, RTE is expected to be the dominant TE mechanism particularly when close to the RTE maximum. Therefore a comparison of the experimental data to the RTE calculations should provide valuable information as to the dominant processes involved in the production of these states.

In figures 3(c) and (d), the ratios R_g and r_g of experiment to RTE theory (computed using equation (7) of [8]) from our data of boron and fluorine beams as well as from fitted areas to the unsubtracted spectra of [20] (figure 2) are plotted as a function of the collision energy. For both ground state ratios R_g and r_g, agreement is not as good as that for the metastable state ratios. In particular, for r_g, a consistent disagreement is particularly noticeable and quite unexpected. Unfortunately, in the case of fluorine the data could not lead to an evaluation of r_g since the $^2P_-$ peak is practically absent.

We note that both ratios r_m and r_g involve the same ratio of Auger yields, i.e. $\xi[^2P_-]/\xi[^2P_+]$ and therefore if r_m is in

agreement with theory the observed disagreement between $r_{g\,\mathrm{theo}}$ and $r_{g\,\mathrm{exp}}$ can not be justified on the grounds of possibly incorrect Auger yields. Thus, any discrepancy between theory and experiment in r_g, assuming that the RTE calculation is valid and the IA is accurate and applicable, must be due to additional NTE*g* processes that come into play. Spin statistical arguments, as the ones already used for the expected ratios of R_m, can also be applied to NTE*g* and show that the probability of transfer in NTE in going from the $1s^2$ He-like ground state to the $^2P_-$ and $^2P_+$ Li-like states can be expected to occur in a 3 : 1 ratio (i.e. the ratio of $^2P_-$: $^2P_+$ formed by NTE*g*) which is seen to be the inverse of the value of the ratio for the probabilities of these two states to be formed by single electron capture from the metastable. However, this can be seen to be consistent with an analogous calculation of capture, but now into the excited $1s2s\ ^1S$ or $1s2p\ ^1P$ *singlet* states [39], assumed to be first formed from the ground state by excitation and then followed by capture of a spin-up or spin-down electron into the 2*s* or 2*p*, respectively, to form the $^2P_\pm$ states, as the 2nd step of the NTE*g* process. This is in the right direction of increasing preferentially the $^2P_-$ population and therefore the denominator of r_g. A point that argues against the involvement of additional NTE*g*, is of course, the fact that measurements of R_m for carbon on the much heavier Ne target [20] (for which it is well-known that NTE contributions should be much larger than for light targets sush as H_2 and He), were very similar to the results obtained with H_2. This could mean the correct and full subtraction of all ground state contributions (therefore also of NTEg).

In addition, only the 4 MeV $B^{3+} + H_2$ and the 6 MeV $C^{4+} +$ He collision systems are close to the RTE maximum values where RTE is expected to dominate. At these energies better agreement of $r_{g\,\mathrm{RTE}}$ with $r_{g\,\mathrm{exp}}$ is expected which is clearly not the case for carbon, and marginally so for boron, the difference between the H_2 target and He targets clearly playing some role as it is well known that He gives rise to more NTE*g* than H_2 [4]. The necessity of even better statistics in these measurements is clearly apparent for more secure conclusions about the value of the ratios of $^2P_\pm$ in the overall analysis. Clearly, a proper calculation of NTE*g* is also needed for a more quantitative prediction, but the above arguments show this to be in the right direction. Overall, further work in understanding these seemingly conflicting results is needed and we are in the process of supplying additional experimental results in the APAPES [38] project underway.

3.4. Advantages and applicability of the technique

From the results of equations (25)–(28), it becomes clear that our technique offers the following three *significant* advantages: (a) It replaces the need for a measurement with a *pure* ground state beam, usually hard to realize in practice and only possible in a rather narrow collision energy window, by the relatively easier and more broadly applicable requirement of two measurements using mixed state beams with *different* values of metastable fraction $f_{^3S}$. (b) It bypasses the need for determining $f_{^3S}$, thus eliminating a considerable additional source of error in R_m and the other three ratios. It is reminded that differences in metastable content can be readily judged by inspection of the $^4P/^2D$ line area ratio. (c) It also bypasses the need for mutually *normalized* spectra, as it involves only *ratios* of areas of peaks from the *same* spectrum, literally using only the 'raw data' of each spectrum. Thus, the accuracy in the determination of the four ratios R_m, r_m, R_g, r_g is seen to depend *just* on the counting statistics attainable in the measurements.

To apply our technique the following two conditions are important: (i) The ^4P state be populated strongly from *only* the metastable $1s2s\ ^3S$ state, and (ii) the ^2D state be populated strongly from *only* the $1s^2$ ground state. These two conditions are expected to be satisfied in collisions with low-*Z* targets such as H_2 or He [8]. Aside from these, however, the method's critical requirement is that the two spectra used must be obtained in measurements with beams having *appreciably* different $f_{^3S}$ content. The larger the differences in this metastable content the more robust and accurate should be the results. Clearly, in the case when one measurement can be performed with near zero metastable fraction, as already mentioned not always possible, this should correspond to the most accurate results when using our equations (25)–(27). This extreme and optimal situation is investigated in appendix B.

4. Summary and conclusions

We report on new results on the value of the ratio $R_m = \sigma_{T_{2p}}(^4P)/(\sigma_{T_{2p}}(^2P_+) + \sigma_{T_{2p}}(^2P_-))$ of state production cross sections formed by 2*p* electron transfer to the $1s2s\ ^3S$ metastable beam component obtained from previously published Auger electron spectra for collisions of 4.5 MeV $B^{3+}(1s^2\ ^1S, 1s2s\ ^3S)$ and 25.3 MeV $F^{7+}(1s^2\ ^1S, 1s2s\ ^3S)$ with H_2 targets. Our new results were obtained using a new method that utilizes two independent measurements of the same projectile Auger spectrum, but with quite different $1s2s\ ^3S$ metastable fraction in the ion beam of each measurement. Its comparative advantage lies in the fact that it allows for the determination of R_m with considerable reduction of experimental uncertainty, even in cases where it is not possible to obtain a pure ground state He-like ion beam, as required in older methods. Our results for boron show a clear departure from the expected theoretical value of $R_m = 2$, in support of earlier indications for carbon [20, 21] and fluorine [22], with no clear explanation to date. In addition to our results on R_m, we also present for the first time results on the related ratio, $r_m = \sigma_{T_{2p}}(^2P_+)/\sigma_{T_{2p}}(^2P_-)$, which is found to be in fairly good agreement with its theoretically predicted value of $r_m = 3$. Moreover, our method also allows us to determine the additional ratios of $^2D/^2P$ and $^2P_+/^2P_-$ populations produced from the *ground* state beam component. These ratios when compared to RTE calculations—expected to be the dominant contributor—result in unexpected disagreement, suggesting the possibility of an additional active NTE*g* process.

With the addition of these new results for boron and fluorine to those of carbon, we have shown that an adequate

explanation of the observed discrepancies between theory and experiment is still missing. The determination of R_m is important since any deviations from its fundamental theoretical value of *two* indicates the existence of mechanisms at play either awaiting to be discovered, or known but thought to be unimportant or even not well understood. Thus, it opens up a window for exploring such hidden processes as for example the proposed enhancement mechanisms of selective cascade feeding and/or dynamic Pauli exchange. Consequently, there still seems to be a clear need to further extend this isoelectronic investigation over the entire first row of the periodic table and possibly even to higher Z atomic species, providing high quality Auger electron spectra in a systematic approach. In addition, the inclusion of heavier gas targets such as Ne and Ar in our method and comparisons to H_2 and He will shed further light on the role of the NTE processes in populating the Li-like states. From our current understanding, in heavier targets, NTEm can be expected to noticeably enhance the population of the ^4P and ^2P states, while NTEg is expected to considerably affect the ^2P and ^2D populations especially at collision energies far from the RTE maximum. However, accurate NTE calculations are clearly required to reach quantitative results and to support corresponding measurements. Finally, cascade contributions will need to be computed for all ions utilized in any such measurements including their effect on the solid angle correction factor for the long-lived $1s2s2p\ ^4P$ state. Theoretical account of NTE contributions both from the ground and the metastable states would be particular useful together with other basic theoretical support on atomic structure of Li- and He-like ionic states. Currently, we are working towards these goals with our ZAPS setup now in full operation within the APAPES project [44] at the Athens 5.5 MV tandem accelerator of the NCSR Demokritos.

Acknowledgments

Many thanks to Tom Kirchner and Alfred Müller for critically reading the original manuscript, to Tom Gorczyca and Elmar Träbert for providing atomic structure information and/or other helpful clarifications and to Ioannis Madesis for help with the data analysis.

Appendix A. Determination of cross sections $\mathrm{d}\sigma_m[x]/\mathrm{d}\Omega'$ and $\mathrm{d}\sigma_g[x]/\mathrm{d}\Omega'$

Writing out the eight equations represented by the system of equations (12) (the notation $^2P_\pm$ represents two different states) for each of the two measurements (two different spectra) we have in detail for each x : ^4P, $^2P_\pm$ and ^2D,

Spectrum 1:

$$(1 - f_{^3S}^{[1]})\frac{\mathrm{d}\sigma_g[x]}{\mathrm{d}\Omega'} + f_{^3S}^{[1]}\frac{\mathrm{d}\sigma_m[x]}{\mathrm{d}\Omega'} = \frac{\mathrm{d}\sigma_1[x]}{\mathrm{d}\Omega'}. \tag{A.1}$$

Spectrum 2:

$$(1 - f_{^3S}^{[2]})\frac{\mathrm{d}\sigma_g[x]}{\mathrm{d}\Omega'} + f_{^3S}^{[2]}\frac{\mathrm{d}\sigma_m[x]}{\mathrm{d}\Omega'} = \frac{\mathrm{d}\sigma_2[x]}{\mathrm{d}\Omega'}. \tag{A.2}$$

The above system of eight nonlinear equations in ten unknowns (each of the four $\frac{\mathrm{d}\sigma_g[x]}{\mathrm{d}\Omega'}$, four $\frac{\mathrm{d}\sigma_m[x]}{\mathrm{d}\Omega'}$ for x: ^4P, $^2P_\pm$, ^2D states and the two unknown fractions $f_{^3S}^{[1]}, f_{^3S}^{[2]}$) cannot in general be solved. However, under the basic assumption that the ^4P state *cannot* be populated from the *ground* state beam and the ^2D state *cannot* be populated from the *metastable* beam component means that $\frac{\mathrm{d}\sigma_g[^4P]}{\mathrm{d}\Omega'} = 0$ and $\frac{\mathrm{d}\sigma_m[^2D]}{\mathrm{d}\Omega'} = 0$, and when applied to equations (A.1) and (A.2) reduces our system to eight equations with eight unknowns ($^2P_\pm$ counts as two equations):

Spectrum 1:

$$f_{^3S}^{[1]}\frac{\mathrm{d}\sigma_m[^4P]}{\mathrm{d}\Omega'} = \frac{\mathrm{d}\sigma_1[^4P]}{\mathrm{d}\Omega'}, \tag{A.3}$$

$$(1 - f_{^3S}^{[1]})\frac{\mathrm{d}\sigma_g[^2P_\pm]}{\mathrm{d}\Omega'} + f_{^3S}^{[1]}\frac{\mathrm{d}\sigma_m[^2P_\pm]}{\mathrm{d}\Omega'} = \frac{\mathrm{d}\sigma_1[^2P_\pm]}{\mathrm{d}\Omega'}, \tag{A.4}$$

$$(1 - f_{^3S}^{[1]})\frac{\mathrm{d}\sigma_g[^2D]}{\mathrm{d}\Omega'} = \frac{\mathrm{d}\sigma_1[^2D]}{\mathrm{d}\Omega'}. \tag{A.5}$$

Spectrum 2:

$$f_{^3S}^{[2]}\frac{\mathrm{d}\sigma_m[^4P]}{\mathrm{d}\Omega'} = \frac{\mathrm{d}\sigma_2[^4P]}{\mathrm{d}\Omega'}, \tag{A.6}$$

$$(1 - f_{^3S}^{[2]})\frac{\mathrm{d}\sigma_g[^2P_\pm]}{\mathrm{d}\Omega'} + f_{^3S}^{[2]}\frac{\mathrm{d}\sigma_m[^2P_\pm]}{\mathrm{d}\Omega'} = \frac{\mathrm{d}\sigma_2[^2P_\pm]}{\mathrm{d}\Omega'}, \tag{A.7}$$

$$(1 - f_{^3S}^{[2]})\frac{\mathrm{d}\sigma_g[^2D]}{\mathrm{d}\Omega'} = \frac{\mathrm{d}\sigma_2[^2D]}{\mathrm{d}\Omega'}. \tag{A.8}$$

We note that equations (A.3), (A.6) and (A.5), (A.8) now becomes a system of *four* equations in *four* unknowns with the solution:

$$\frac{\mathrm{d}\sigma_m[^4P]}{\mathrm{d}\Omega'} = \frac{\mathrm{d}\sigma_2[^4P]\,\mathrm{d}\sigma_1[^2D] - \mathrm{d}\sigma_1[^4P]\,\mathrm{d}\sigma_2[^2D]}{\mathrm{d}\sigma_1[^2D] - \mathrm{d}\sigma_2[^2D]}, \tag{A.9}$$

$$\frac{\mathrm{d}\sigma_g[^2D]}{\mathrm{d}\Omega'} = \frac{\mathrm{d}\sigma_2[^2D]\,\mathrm{d}\sigma_1[^4P] - \mathrm{d}\sigma_1[^2D]\,\mathrm{d}\sigma_2[^4P]}{\mathrm{d}\sigma_1[^4P] - \mathrm{d}\sigma_2[^4P]}, \tag{A.10}$$

$$f_{^3S}^{[i]} = \frac{\mathrm{d}\sigma_i[^4P](\mathrm{d}\sigma_2[^2D] - \mathrm{d}\sigma_1[^2D])}{\mathrm{d}\sigma_1[^4P]\mathrm{d}\sigma_2[^2D] - \mathrm{d}\sigma_2[^4P]\mathrm{d}\sigma_1[^2D]}, \tag{A.11}$$

where we have used the short hand $\mathrm{d}\sigma_i[x] \equiv \mathrm{d}\sigma_i[x]/\mathrm{d}\Omega'$. Using the results of equation (A.11) for the metastable fractions $f_{^3S}^{[i]}$ (with $i = 1, 2$) in equations (A.4) and (A.7) we can immediately solve this system, also of four equations with four unknowns, to obtain the remaining unknowns. From the symmetry of the equations it can be readily seen that all solutions have the general form:

$$\frac{\mathrm{d}\sigma_m[x]}{\mathrm{d}\Omega'} = \frac{\mathrm{d}\sigma_2[x]\,\mathrm{d}\sigma_1[^2D] - \mathrm{d}\sigma_1[x]\,\mathrm{d}\sigma_2[^2D]}{\mathrm{d}\sigma_1[^2D] - \mathrm{d}\sigma_2[^2D]} \quad \text{for } x:\ ^2P_\pm,\ ^4P,\ ^2D \tag{A.12}$$

$$\frac{\mathrm{d}\sigma_g[x]}{\mathrm{d}\Omega'} = \frac{\mathrm{d}\sigma_2[x]\,\mathrm{d}\sigma_1[^4P] - \mathrm{d}\sigma_1[x]\,\mathrm{d}\sigma_2[^4P]}{\mathrm{d}\sigma_1[^4P] - \mathrm{d}\sigma_2[^4P]} \tag{A.13}$$

with the metastable fractions given by:

$$f_{^3S}^{[i]} = \frac{\mathrm{d}\sigma_i[^4P](\mathrm{d}\sigma_2[^2D] - \mathrm{d}\sigma_1[^2D])}{\mathrm{d}\sigma_1[^4P]\mathrm{d}\sigma_2[^2D] - \mathrm{d}\sigma_2[^4P]\mathrm{d}\sigma_1[^2D]} \quad \text{for } i = 1, 2. \tag{A.14}$$

Equations (A.12) and (A.13) are seen to also satisfy the main assumption $\frac{\mathrm{d}\sigma_g[^4P]}{\mathrm{d}\Omega'} = \frac{\mathrm{d}\sigma_m[^2D]}{\mathrm{d}\Omega'} = 0$.

We finally note that the ratio of the metastable fractions in the two measurements is given directly from equation (A.11) as:

$$\frac{f_{^3S}^{[1]}}{f_{^3S}^{[2]}} = \frac{\mathrm{d}\sigma_1[^4P]}{\mathrm{d}\sigma_2[^4P]} = \frac{\kappa_2}{\kappa_1}\frac{N_1^e[^4P]}{N_2^e[^4P]} \tag{A.15}$$

from which it is clear that the metastable fraction is proportional to the intensity of the *normalized* ^4P line in the electron spectra as expected. Even in the case where both measurements are performed on the same apparatus, the ratio κ_2/κ_1 drops out only if the *same* total number of ions N_I (see equation (6)) is used in both measurements assuming all other parameter values remain the same.

Appendix B. $R_{m\,\mathrm{exp}}$ in the case of $f_{^3S}^{[2]} = 0$

In this case the 2nd measurement is performed with zero metastable fraction $f_{^3S}^{[2]} = 0$, i.e. with a *pure* ground state beam or no ^4P peak evident. Then, the first (mixed beam measurement) spectrum is normalized to the ^2D line (which can be produced only from the ground state) of the 2nd pure ground state spectrum and the $^2P_\pm$ SDCS [24, 25] (or even DDCS) from the metastable beam component can be obtained by subtraction (without any need for the more general case presented the more general case presented in appendix A) directly giving:

$$\frac{\mathrm{d}\sigma_m[^2P_\pm]}{\mathrm{d}\Omega'} = \mathrm{d}\sigma_1[^2P_\pm] - \mathrm{d}\sigma_2[^2P_\pm]\left(\frac{\mathrm{d}\sigma_1[^2D]}{\mathrm{d}\sigma_2[^2D]}\right) \tag{B.1}$$

$$= \mathrm{d}\sigma_1[^2P_\pm] - \mathrm{d}\sigma_2[^2P_\pm](1 - f_{^3S}^{[1]}) \tag{B.2}$$

with the metastable fraction given directly from equation (A.11) with $\mathrm{d}\sigma_2[^4P] = 0$ by:

$$f_{^3S}^{[1]} = 1 - \frac{\mathrm{d}\sigma_1[^2D]}{\mathrm{d}\sigma_2[^2D]} = 1 - \frac{\kappa_2}{\kappa_1}\frac{N_1^e[^2D]}{N_2^e[^2D]} \tag{B.3}$$

with the ratio R_m then given by:

$$R_{m\,\mathrm{exp}} = \frac{\mathrm{d}\sigma_1[^4P]}{\mathrm{d}\sigma_2[^2P](1 - f_{^3S}^{[1]}) - \mathrm{d}\sigma_1[^2P]}. \tag{B.4}$$

Equation (B.4) is the form used to date both in our own collaborations [24, 25], but also by Strohschein *et al* [20] together with equation (B.3) for the metastable fraction. The uncertainty in the determination of $R_{m\,\mathrm{exp}}$, thus depends just on the inherent uncertainties of the parameters in equation (B.4) including any error from the determination of the metastable fraction $f_{^3S}^{[1]}$ which is also seen (equation (B.3)) to depend on the absolute normalization parameters κ_1 and κ_2.

In hindsight and as already shown in our new technique to address the case of $f_{^3S}^{[2]} = 0$ we may just set in the expression for $R_{m\,\mathrm{exp}}$ (equation (21)) $\mathrm{d}\sigma_2[^4P] = 0$ to obtain:

$$R_{m\,\mathrm{exp}} = \frac{\frac{\mathrm{d}\sigma_1[^4P]}{\mathrm{d}\sigma_1[^2D]}}{\frac{\mathrm{d}\sigma_2[^2P]}{\mathrm{d}\sigma_2[^2D]} - \frac{\mathrm{d}\sigma_1[^2P]}{\mathrm{d}\sigma_1[^2D]}} \tag{B.5}$$

which is seen to be identical with expression in equation (B.4) when equation (B.3) is also used. However, now it is clear that the metastable fraction need not be determined explicitly and equation (B.5) includes only *ratios of peaks from the same spectrum* and therefore *independent* of the absolute normalization parameters κ_1 and κ_2 which cancel.

Even though the form of R_m given in equation (B.4) could be considered intuitively more appealing, since the denominator is clearly presented as the difference between the mixed beam measurement $\mathrm{d}\sigma_1[^2P]$ minus the *normalized* (at the ^2D line via factor κ_1/κ_2) ground state contribution expressed by $(1 - f_{^3S}^{[1]})\mathrm{d}\sigma_2[^2P]$, where $(1 - f_{^3S}^{[1]})$ is the ground state component of the mixed beam in measurement 1, it can be of *lower overall accuracy* than the form of R_m given by equation (25), when the metastable beam fraction $f_{^3S}^{[1]}$ is *not determined simultaneously from the same spectra* using equation (B.3), but taken from the literature (e.g. [26, 28]) as done in the case of the older fluorine data taken with the tandem PPA. In this case, the ratio κ_1/κ_2 does not necessarily always cancel (for example the overall (usually detector) efficiency $\overline{\eta}$ in equation (8) could be quite different in measurements from different time periods even if the setup is otherwise exactly the same) and the overall uncertainly $\Delta\kappa_i$ in the κ_i values, as well as the error Δf in the determination of $f_{^3S}^{[1]}$ could in principle constitute *additional* sources of absolute uncertainty in the value of R_m, not present though in the original two-different fraction formulation of R_m given via equations (25) and (B.5).

References

[1] Stolterfoht N 1987 *Phys. Rep.* **146** 315
[2] Zouros T J M and Lee D H 1997 *Accelerator-Based Atomic Physics Techniques and Applications* (*American Institute of Physics Conference Series*) ed S M Shafroth and J C Austin (Woodbury, NY: AIP) pp 426–79 ch 13
[3] Tanis J A *et al* 2004 *Phys. Rev. Lett.* **92** 133201
[4] Lee D H *et al* 1991 *Nucl. Instrum. Methods Phys. Res.* B **56/57** 99
[5] Mack M and Niehaus A 1987 *Nucl. Instrum. Methods Phys. Res.* B **23** 109
[6] Mack M and Niehaus A 1987 *Nucl. Instrum. Methods Phys. Res.* B **23** 116
[7] Graham W G, Fritsch W, Hahn Y and Tanis J (ed) 1992 *Recombination of Atomic Ions* (*NATO Ions Advanced Study Institute Series B: Physics* vol 296) (New York: Plenum)
[8] Lee D H *et al* 1991 *Phys. Rev.* A **44** 1636
[9] Benis E P *et al* 2003 *J. Phys. B: At. Mol. Opt. Phys.* **36** L341
[10] Závodszky P A *et al* 2001 *Phys. Rev. Lett.* **87** 033202

[11] Alnaser A S *et al* 2002 *Phys. Rev.* A **65** 042709
[12] Borovik A Jr *et al* 2009 *J. Phys. B: At. Mol. Opt. Phys.* **42** 025203
[13] Renwick A C *et al* 2009 *J. Phys. B: At. Mol. Opt. Phys.* **42** 175203
[14] Schlummer T *et al* 2015 *J. Phys. B: At. Mol. Opt. Phys.* **48** 144033
[15] Cui Z *et al* 2013 *Nucl. Fusion* **53** 093001
[16] Liu L, Jakimovski D, Wang J G and Janev R K 2012 *J. Phys.* **45** 225203
[17] Trassinelli M *et al* 2012 *J. Phys. B: At. Mol. Opt. Phys.* **45** 085202
[18] Nandi T *et al* 2012 *J. Quant. Spectrosc. Radiat. Transfer* **113** 783
[19] Lin Y-C and Ho Y 2014 *Can. J. Phys.* **93** 646
[20] Strohschein D *et al* 2008 *Phys. Rev.* A **77** 022706
[21] Röhrbein D, Kirchner T and Fritzsche S 2010 *Phys. Rev.* A **81** 042701
[22] Zouros T J M, Sulik B, Gulyas L and Tokesi K 2008 *Phys. Rev.* A **77** 050701
[23] Benis E P *et al* 2004 *Phys. Rev.* A **69** 052718
[24] Benis E P, Zamkov M, Richard P and Zouros T J M 2002 *Phys. Rev.* A **65** 064701
[25] Zamkov M, Benis E P, Richard P and Zouros T J M 2002 *Phys. Rev.* A **65** 062706
[26] Terasawa M *et al* 1983 *Phys. Rev.* A **27** 2868
[27] Snowdon K. J, Havener C. C, Meyer F. W, Overbury S, Zehner D. M and Heiland W 1988 *Rev. Sci. Instrum.* **59** 902
[28] Dillingham T R *et al* 1984 *Phys. Rev.* A **29** 3029
[29] Dijkkamp D *et al* 1983 *J. Phys. B: At. Mol. Opt. Phys.* **16** L343
[30] Brazuk A. 1985 *Nucl. Instrum. Methods Phys. Res.* B **9** 442
[31] Druetta M., Martin S. and Desesquelles J. 1987 *Nucl. Instrum. Methods Phys. Res.* B **23** 268
[32] Druetta M., Bouchama T. and Martin S. 1989 *Nucl. Instrum. Methods Phys. Res.* B **40** 50
[33] Welton R. F., Moran T. F. and Thomas E. W. 1991 *J. Phys. B: At. Mol. Opt. Phys.* **24** 3815
[34] Itoh A *et al* 1985 *Phys. Rev.* A **31** 684
[35] Wojdyr M 2010 *J. Appl. Crystallogr.* **43** 1126
[36] Doukas S *et al* 2015 *Rev. Sci. Instrum* **86** 043111
[37] Lee D H 1990 *PhD Dissertation* Kansas State University
[38] Benis E P 2001 *PhD Dissertation* Department of Physics, University of Crete
[39] Benis E P *et al* 2006 *Phys. Rev.* A **73** 029901
[40] Benis E P, Doukas S and Zouros T J M 2016 *Nucl. Instrum. Methods Phys. Res.* B **369** 83
[41] Kirchner T 2016 private communication
[42] Parente F and Santos J P 2016 private communication
[43] Madesis I *et al* 2015 *J. Phys: Conf. Ser.* **635** 052082
[44] APAPES—Atomic Physics with Accelerators: Projectile Electron Spectroscopy, http://apapes.physics.uoc.gr